1、提出了一种电动汽车（EV）的协调充电调度方法。
2、在所提出的方法中估计了电动汽车用户充电需求的紧迫性。
3、根据充电需求的紧迫性为电动汽车选择最佳充电模式。
4、该模型可以实现微电网的削峰填谷。
5、该模型的性能在不同的充电模式和EV规模下进行评估。

Energy 213 (2020) 118882

Contents lists available at ScienceDirect

Energy

journal homepage: www.elsevier.com/locate/energy

A coordinated charging scheduling method for electric vehicles considering different charging demands

Kaile Zhou [a, b, c, d, *], Lexin Cheng [a, b], Lulu Wen [a, b], Xinhui Lu [a, b, c, d], Tao Ding [a, b, c, d]

[a] School of Management, Hefei University of Technology, Hefei, 230009, China
[b] Key Laboratory of Process Optimization and Intelligent Decision-making, Ministry of Education, Hefei University of Technology, Hefei, 230009, China
[c] Intelligent Interconnected Systems Laboratory of Anhui Province (Hefei University of Technology), Hefei, 230009, China
[d] Ministry of Education Engineering Research Center for Intelligent Decision-making & Information System Technologies, Hefei, 230009, China

ARTICLE INFO

Article history:
Received 13 May 2020
Received in revised form
20 August 2020
Accepted 16 September 2020
Available online 22 September 2020

Keywords:
Electric vehicles
Coordinated charging
Optimal load scheduling
Charging demand

ABSTRACT

The uncoordinated charging of large amounts of electric vehicles (EVs) can lead to a substantial surge of peak loads, which will further influence the operation of power system. Therefore, this study proposed a coordinated charging scheduling method for EVs in microgrid to shift load demand from peak period to valley period. In the proposed method, the charging mode of EVs was selected based on a charging urgency indicator, which can reflect different charging demand. Then, a coordinated charging scheduling optimization model was established to minimize the overall peak-valley load difference. Various constraints were considered for slow-charging EVs, fast-charging EVs, and microgrid operation. Furthermore, Monte Carlo Simulation (MCS) was used to simulate the randomness of EVs. The results have shed light on both the charging modes selection for EV owners and peak shaving and valley filling for microgrid operation. As a result, this model can support more friendly power supply-demand interaction to accommodate the increasing penetration of EVs and the rapid development of flexible microgrid.

1. Introduction

Electric vehicles (EVs) are eco-friendly as they consume electrical energy and generate nearly zero pollutant emissions [1–3]. Therefore, EVs provide an alternative option for developing cleaner transportation systems and offer great potential for sustainable transport development [4,5]. Meanwhile, EVs can be more easily incorporated into intelligent transportation systems to enhance smart transportation services [6,7].

Nevertheless, the development of EVs faces some challenges. The limitation of battery technology and the shortage of charging infrastructures are some of the crucial problems [6,8]. Besides, the degradation of EV battery and the high cost of EV battery are commonly regarded as the major concerns of EV adoption [9–12]. The fast-charging technology and the charging station planning also need to be improved [13,14]. In addition to technological challenges, management and business-related issues also affect the interaction between EVs and the main power grid or microgrid, thereby impeding the penetration of large-scale EVs [15–18]. For example, large-scale uncoordinated charging of EVs can bring great pressure to the power supply and thus influence the safety and stability of power system. To address this problem, it is necessary to optimize the charging of large-scale EVs [19].

Currently, there have been some research efforts regarding the optimization of EV charging scheduling [20]. However, existing studies mainly focused on the supply side to achieve the lowest operation cost and the minimum peak-valley load difference. The specific charging demands of EV owners were usually not taken into account for EV charging scheduling. In the actual situation, the charging demands of EV owners are usually different, especially in the case that some EVs have urgent charging demands. To fill this gap, this study proposed a coordinated charging scheduling method for EVs while considering different charging demands of EV owners.

The main contributions of this paper are as following. First, the proposed method considers the urgency of EV charging demand, which was determined by a charging urgency indicator (CUI). Second, all the EVs were scheduled according to different charging demands rather than as a whole. Third, to demonstrate the effectiveness of the proposed method in actual situation, the

* Corresponding author. School of Management, Hefei University of Technology, Hefei, 230009, China.
E-mail address: zhoukaile@hfut.edu.cn (K. Zhou).

https://doi.org/10.1016/j.energy.2020.118882
0360-5442/

uncertainty of EV charging behaviour was taken into consideration by using two different charging patterns of EVs in simulations. The results showed that the proposed method can shift load demand from peak period to valley period and minimize the total peak-valley load difference by scheduling EV charging coordinately, thereby contributing to improving the safety and reliability of microgrid.

The rest of this paper is organized as follows. Section 2 presents the literature review. Section 3 introduces the proposed coordinated EVs charging scheduling method. The detailed simulation results and discussions are provided in Section 4, and Section 5 gives the conclusions.

2. Literature review

Substantial research exists regarding the optimal dispatch methods for addressing the EV charging scheduling problem [21–23]. Many studies have explored such problem by using the decentralized charging methods or centralized methods. Decentralized valley-filling charging strategies were proposed in Refs. [24–27]. In decentralized approaches, day-ahead pricing schemes are usually used to change EV owners' charging behaviour for saving costs [28–30]. This releases the pressure of the power system during the rush hours. Nevertheless, such pricing mechanism may lead to the emergence of new charging peaks as the charging choices are made by drivers independently. Besides, decentralized charging methods need two prerequisites: (a) the EV owners are sensitive to the pricing scheme and will change their EV charging patterns; and (b) the price information has to be announced to the EV drivers in time.

In centralized approaches, the EV aggregator can collect charging information of the EV and then arrange the EV charging periods directly in a centralized manner. From a long-term perspective, the centralized method is more significant compared to the decentralized approach for EV charging scheduling [31,32]. Zhang et al. [27] and Zheng et al. [33] pointed out that EV aggregator scheduling EV charging behaviour in a centralized way can ensure the utilization of surplus power during the valley times. In addition, related charging information is provided by EV owners when EVs are connected to the microgrid [33–35]. Nevertheless, the urgency of each EV is was not well measured and considered in scheduling in the majority of previous studies. If all the EVs are considered as a whole in the charging scheduling, the urgent charging demand of EV owners cannot be satisfied.

There are several different objective functions adopted in the centralized approaches for EV charging scheduling, including minimizing the power losses [28,36], controlling the trading risks [37,38], maximizing the operation profits [23], maximizing the integration of renewable energies [39,40], minimizing the peak load [41], and minimizing the power load variance [35,42]. In previous studies, several algorithms have been used to solve these optimization problems, such as the interior point method [43], the particle swarm optimization (PSO) algorithm [20,44–46], the genetic algorithm [47], and the improved PSO algorithm [20,46]. However, it should be noted that the computational complexities will increase dramatically when using these approaches to optimize the scheduling of large-scale EVs charging. These optimization methods may also fail to find global optimal solution.

3. Model

3.1. General description

This study aims to develop a coordinated charging scheduling method that can achieve peak shaving and valley filling for the microgrid. In the EV charging scheduling process, the EV aggregator collects charging information and implements EV charging scheduling. When the EV is connected to the microgrid, EV owners set the charging information and send it to the EV aggregator. The information includes the arrival time and departure time, the State of Charge (SOC) when the EV is connected to the microgrid, the lower SOC for the charging demand of EV and the upper SOC for the safety of the EV battery [34,35].

Based on the collected information, the coordinated charging scheduling method can be implemented. The first step is setting the length and number of time slots. Next, the EV arrival time and departure time are normalized into time slots. Then, an EV CUI is defined to distinguish whether the charging demand of the EV is urgent, and two charging modes are available to EV owners.

In the proposed EVs charging scheduling model, the charging state is a state variable that is defined to reflect whether the EV charges at a certain time slot. The objective of the proposed coordinated charging scheduling method is minimizing the peak-valley load difference of the microgrid. Fig. 1 presents the framework diagram of the proposed EVs charging scheduling model.

3.2. Charging and discharging time

Considering the charging habits of the EV owners, the regular patterns of EV charging can be classified into two charging patterns: home-charging and public-charging patterns [33].

In the home-charging pattern, the EV owners starts charging when arriving home after work and end charging when they get ready to go work. The EV arrival time t_{1c} and departure time t_{1dis} follow normal distribution which can be expressed as:

$$f(t_{1c})=\begin{cases}\dfrac{1}{\sqrt{2\pi}\sigma_{1t_c}}\exp\left(-\dfrac{(t_{1c}+24-\mu_{1t_c})^2}{2{\sigma_{1t_c}}^2}\right) & 0<t_{1c}\le\mu_{1t_c}-12\\ \dfrac{1}{\sqrt{2\pi}\sigma_{1t_c}}\exp\left(-\dfrac{(t_{1c}-\mu_{1t_c})^2}{2{\sigma_{1t_c}}^2}\right) & \mu_{1t_c}-12<t_{1c}\le 24\end{cases} \tag{1}$$

$$f(t_{1dis})=\begin{cases}\dfrac{1}{\sqrt{2\pi}\sigma_{1t_{dis}}}\exp\left(-\dfrac{(t_{1dis}-\mu_{1t_{dis}})^2}{2{\sigma_{1t_c}}^2}\right) & 0<t_{1dis}\le\mu_{1t_{dis}}+12\\ \dfrac{1}{\sqrt{2\pi}\sigma_{1t_{dis}}}\exp\left(-\dfrac{(t_{1dis}-24-\mu_{1t_{dis}})^2}{2{\sigma_{1t_c}}^2}\right) & \mu_{1t_{dis}}+12<t_{1dis}\le 24\end{cases} \tag{2}$$

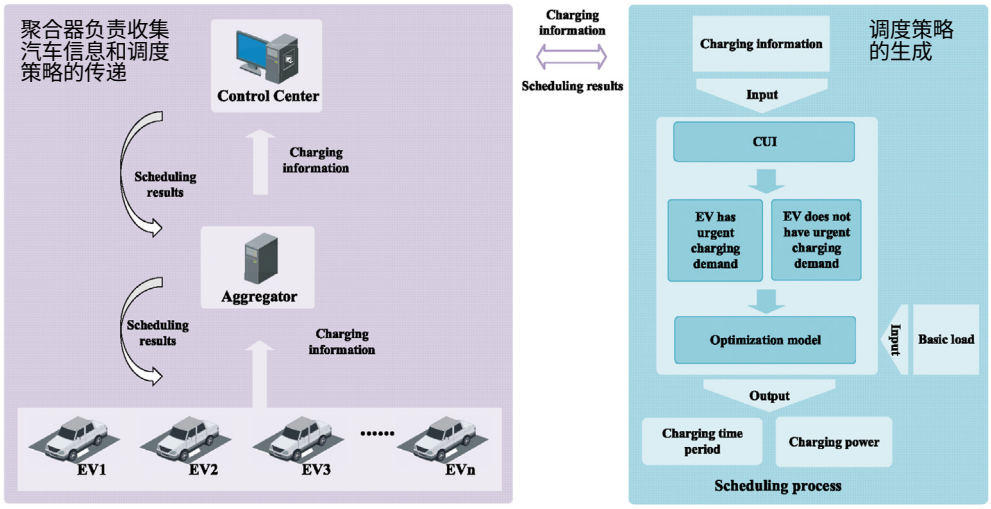

Fig. 1. Framework diagram of the proposed EVs charging scheduling model.

where $\mu_{1t_c} = 18$, $\sigma_{1t_c} = 3.3$, $\mu_{1t_{dis}} = 8$, and $\sigma_{1t_{dis}} = 3.24$ [20].

In the public-charging pattern, EV owners starts charging when arriving at workplaces in the morning and then finish charging after work. The EV arrival time t_{2c} and departure time t_{2dis} also follow normal distribution which can be expressed as:

$$f(t_{2c}) = \begin{cases} \frac{1}{\sqrt{2\pi}\sigma_{2t_c}} \exp\left(-\frac{(t_{2c} - \mu_{2t_c})^2}{2\sigma_{2t_c}^2} \right) & 0 < t_{2c} \le \mu_{2t_c} + 12 \\ \frac{1}{\sqrt{2\pi}\sigma_{2t_c}} \exp\left(-\frac{(t_{2c} - 24 - \mu_{2t_c})^2}{2\sigma_{2t_c}^2} \right) & \mu_{2t_c} + 12 < t_{2c} \le 24 \end{cases} \tag{3}$$

$$f(t_{2dis}) = \begin{cases} \frac{1}{\sqrt{2\pi}\sigma_{2t_{dis}}} \exp\left(-\frac{(t_{2dis} + 24 - \mu_{2t_{dis}})^2}{2\sigma_{2t_c}^2} \right) & 0 < t_{2dis} \le \mu_{2t_{dis}} - 12 \\ \frac{1}{\sqrt{2\pi}\sigma_{2t_{dis}}} \exp\left(-\frac{(t_{2dis} - \mu_{2t_{dis}})^2}{2\sigma_{2t_c}^2} \right) & \mu_{2t_{dis}} - 12 < t_{2dis} \le 24 \end{cases} \tag{4}$$

where $\mu_{2t_c} = 8.5$, $\sigma_{2t_c} = 3.3$ $\mu_{2t_{dis}} = 17.5$, and $\sigma_{2t_{dis}} = 3.24$ [20].

From above definition, the probability distributions of arrival and departure time of different number EVs under the two charging patterns can be obtained as shown in Fig. 2 and Fig. 3. In Figs. 2 and 3, the red curves are the probability distribution functions (PDFs) of arrival and departure time of EVs, and the histograms indicate the generated data according to the PDFs in MCS method.

From Fig. 2, it can be seen that EV owners arrive home at approximately 18 h and go to work at approximately 8 h in the home-charging pattern. Fig. 3 shows that EV owners usually connect the EV into the microgrid when arriving at their workplace at approximately 8.5 h and disconnect the EV from microgrid after work at approximately 17.5 h in the public-charging pattern. Therefore, the generated data are in accordance with the work characteristics of people in two charging patterns.

3.3. Time slot division

In the scheduling process, the scheduling plan is usually executed by period of time for improving execution efficiency. The scheduling time is divided into several time periods. In the proposed EV charging scheduling model, a day is discretized into 96 time slots and the length of a time slot is 15 min. Then, the arrival time and departure time of each EV can be are expressed as:

$$J_i^c = \left\lceil \frac{t_i^c}{\Delta T} \right\rceil, \ i = 1, 2, \ldots, N. \tag{5}$$

$$J_i^{dis} = \left\lfloor \frac{t_i^{dis}}{\Delta T} \right\rfloor, \ i = 1, 2, \ldots, N. \tag{6}$$

where N represents the number of EVs, i is the index of EV, $i = 1, 2, \ldots, N$, j is the index of time slots of a day, and $j = 1, 2, \ldots, 96$. J_i^c and J_i^{dis} denote the serial number of the time slot when $i-th$ EV is connected to the microgrid and disconnected from the microgrid, respectively, t_i^c and t_i^{dis} denote the arrival time and the departure time of the $i-th$ EV, ΔT represents the length of a time slot, $\left\lceil \frac{t_i^c}{\Delta T} \right\rceil$ is the next integer larger than the results of the division operation, $\left\lfloor \frac{t_i^{dis}}{\Delta T} \right\rfloor$ is the previous integer smaller than the results of the division operation.

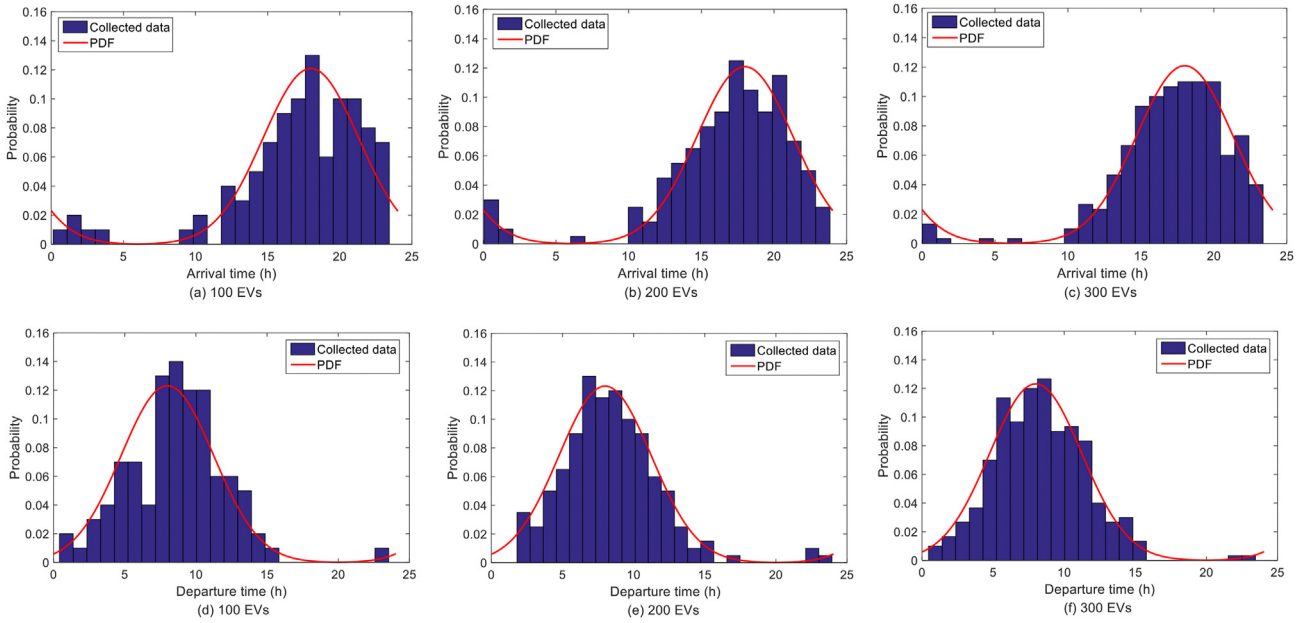

Fig. 2. Simulation results of charging behaviour of three different numbers of EVs in home-charging pattern.

Eq. (5) means that charging behaviour can be arranged after the next integer time slot when the EV is connected to the microgrid at a middle time point of a time slot. Meanwhile, when the EV is disconnected from the microgrid at a middle time point during a time slot, Eq. (6) guarantees that the EV can only be scheduled before the end of the previous integer time slot.

3.4. Charging urgency indicator

In the proposed EV charging scheduling model, all the EVs are scheduled according to their charging demands. In this section, an indicator is defined to reflect the urgency of EV's charging demand.

Based on the arrival time slot J_i^c and departure time slot J_i^{dis}, the whole time slot that the EV is connected to the microgrid can be calculated by:

$$T_i^{\mathrm{Rem}} = J_i^{dis} - J_i^c. \tag{7}$$

where T_i^{Rem} indicates number of remaining time periods that the $i-th$ EV can continue to remain connected to the microgrid, and the charging behaviour and charging scheduling strategy should be arranged in these remaining time periods.

In this study, the CUI is defined as:

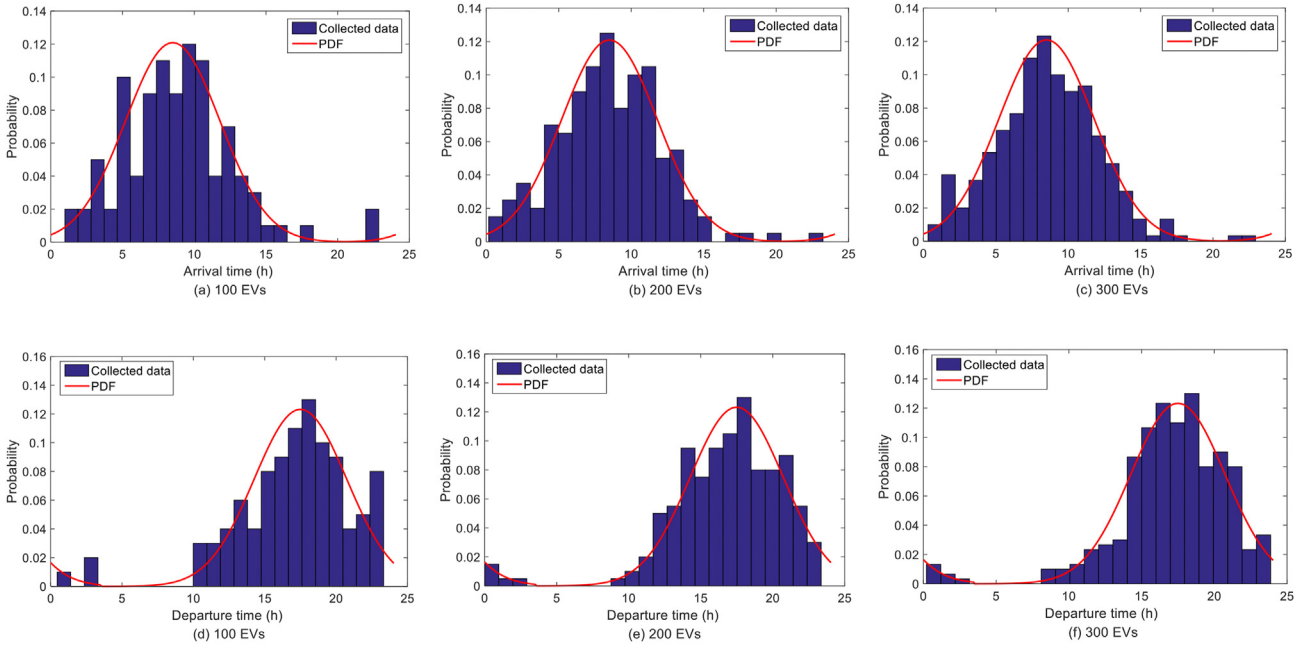

Fig. 3. Simulation results of charging behaviour of three different numbers of EVs in public-charging pattern.

$$CUI_i = \left(T_i^{\mathrm{Rem}} \cdot \triangle T\right) P_{EV}^{slow} \cdot \eta_{EV} - \left(SOC_i^{\min} - SOC_i^{con}\right) \cdot Cap_{EV}^{bat}, \quad i = 1, 2, \ldots\ldots N,\ j = 1, 2, \ldots\ldots 96. \tag{8}$$

where P_{EV}^{slow} is the slow charging power of EVs, η_{EV} denotes the charge efficiency of EVs, $SOC_i^{\min}$ represents the lower bound of SOC when the $i-th$ EV ends its charging behaviour. SOC_i^{con} represents the SOC of the $i-th$ EV when it is connected to the microgrid, Cap_{EV}^{bat} denotes the EV battery capacity. When $CUI_i < 0$, it indicates the charging demand of the $i-th$ EV is urgent. In contrast, when $CUI_i \geq 0$, it means that the charging demand of the $i-th$ EV is not urgent.

3.5. Charging mode selection

Two charging modes of EVs, i.e., fast charging mode and slow charging mode, were considered in the proposed charging scheduling method. Although fast charging provides a short charging time, the current and voltage of the fast charging are relatively high. This will affect the battery life. Therefore, the fast charging model is usually used in some emergency situation [48].

Here, the selection of charging mode is determined by CUI as shown in Eq. (9):

$$P_{EV,i} = \begin{cases} P_{EV}^{fast}, \mathrm{CUI}_i < 0. \\ P_{EV}^{slow}, \mathrm{CUI}_i \geq 0. \end{cases} \tag{9}$$

where P_{EV}^{fast} denotes the fast charging power, and P_{EV}^{slow} denotes the slow charging power. When $CUI_i < 0$, the $i-th$ EV adopts fast charging mode, and when $CUI_i \geq 0$, the $i-th$ EV adopts slow charging mode.

3.6. Optimization model

After parameter preparation and charging mode selection, the optimal model is established. The model consists of three parts: model variables, objective function and constraints for fast-charging EVs and slow-charging EVs. Moreover, the constraints for the microgrid are also added to the model to ensure the microgrid operation.

3.6.1. Charging state variable

In the optimization model, the state variable $x_{i,j}$ is a binary variable. If $x_{i,j} = 0$, it indicates that the $i-th$ EV is not charging during the $j-th$ time slot; if $x_{i,j} = 1$, it means that the $i-th$ EV is charging during the $j-th$ time slot, as shown in Eq. (10).

$$x_{i,j} = \begin{cases} 1, & \text{in charging state.} \\ 2, & \text{not in charging state.} \end{cases} \tag{10}$$

3.6.2. Objective function

This study aims to shift part of load demand from peak period to valley period, and thus to relieve peak load pressure of the microgrid. The total load of the microgrid includes the basic load and the EV charging load, and the EV charging load consists of the loads of fast-charging EVs and slow-charging EVs. Therefore, the total load at the $j-th$ time slot of the coordinated charging scheduling model can be expressed as:

$$P_{T-c}^{j} = P_{con}^{j} + \sum_{i=1}^{N} x_{i,j} \cdot P_{EV,i}. \tag{11}$$

where P_{con}^{j} means the basic load during the $j-th$ time slot, $\sum_{i=1}^{N} x_{i,j} \cdot P_{EV,i}$ indicates the power that is provided for all the EVs in the $j-th$ time slot. If the $i-th$ EV has an urgent charging demand $P_{EV,i}$ is equal to P_{EV}^{fast}; if the $i-th$ EV does not have an urgent charging demand, $P_{EV,i}$ is equal to P_{EV}^{slow}.

The objective of the charging scheduling is to reduce the peak-valley load difference of the microgrid, and it can be expressed as:

$$\min\left(P_{T-c}^{\max} - P_{T-c}^{\min}\right). \tag{12}$$

where $P_{T-c}^{\max}$ and $P_{T-c}^{\min}$ mean the maximal and minimal load demand, respectively.

3.6.3. Constraints for fast-charging EVs

When the $i-th$ EV is regarded as an urgent charging EV, we suppose that $x_{i,j}$ is equal to 1 in every arrival time slot. Therefore, the EV can be charged from the arrival time to the departure time, which assure that the urgent EVs can charge more power in the charging time. Moreover, $x_{i,j}$ is equal to 0 when the EV is disconnected from the microgrid. However, when the degree of an EV's charging urgency is quite small, continuous charging could lead to overcharging with a high charge power P_{EV}^{fast}. To avoid overcharging for fast-charging EVs, the constraint should be set up to limit the charging demand which must be lower than the maximum SOC demand. Considering the two constraints shown above, $x_{i,j}$ is equal to 1 when an EV is connected to the microgrid and maintains the charge state until the EV stop charging. The time slot when EV stop charging is determined by departure time and the time slot during which the maximum SOC demand is satisfied. The constraint for urgent charging EVs can be expressed as:

$$x_{i,j} = \begin{cases} 1, & \text{if } j = J_i^c, \ldots, J_i^{end}. \\ 2, & \text{if others.} \end{cases} \tag{13}$$

where J_i^{end} is the time slot during which the fast-charging EV stop charging, and J_i^{end} can be expressed as:

$$J_i^{end} = \min\left\{J_i^{dis}, \left\lfloor \frac{\left(SOC_i^{\max} - SOC_i^{con}\right) \cdot Cap_{EV}^{Bat}}{P_{EV}^{fast} \cdot \eta_{EV} \cdot \Delta T} \right\rfloor + J_i^c \right\}. \tag{14}$$

where $SOC_i^{\max}$ is the maximum SOC demand, $\frac{\left(SOC_i^{\max} - SOC_i^{con}\right) \cdot Cap_{EV}^{Bat}}{P_{EV}^{fast} \cdot \eta_{EV} \cdot \Delta T}$ denotes charging time slots of the EV that need to satisfy the maximum SOC demand, $\left\lfloor \frac{\left(SOC_i^{\max} - SOC_i^{con}\right) \cdot Cap_{EV}^{Bat}}{P_{EV}^{fast} \cdot \eta_{EV} \cdot \Delta T} \right\rfloor$ denotes the previous integer smaller than the results of the division operation, and this avoids the overcharge of an EV in the next integer.

3.6.4. Constraints for slow-charging EVs

Due to the diversity of charging demands for EV owners, each EV has a minimum SOC demand and a maximum SOC demand to avoid an overcharge. For slow-charging EVs, their minimum SOC demand must be satisfied when EV is disconnected from the microgrid, which can be expressed as follows:

$$SOC_i^{\min} \le SOC_i^{dis} \le SOC_i^{\max}. \tag{15}$$

where the SOC_i^{dis} is the SOC when the $i-th$ EV is disconnected from the microgrid, and it can be calculated by:

$$SOC_i^{dis} = SOC_i^{con} + \frac{\sum_{j=j_i^c}^{j_i^{dis}} \left(\triangle T \cdot P_{EV}^{slow} \cdot x_{i,j} \cdot \eta_{EV} \right)}{Cap_{EV}^{Bat}}. \tag{16}$$

where $x_{i,j}$ includes total number of the slow-charging EVs, and SOC_i^{con} is the SOC when the $i-th$ EV is connected to the microgrid.

The second constraint for slow-charging EVs is related to the scheduling time. The charging behaviour only can be scheduled in the period that the EV is connecting in the microgrid. Therefore, the charging state $x_{i,j}$ must equal to 0, when the slow-charging EV is not connected to the microgrid. It should be noted that the scheduling plan cannot be executed when the EV is disconnected from the microgrid.

3.6.5. Constraint for the microgrid

The objective function is to reduce the peak-valley difference of the total load, but it cannot ensure that the coordinated result of the peak value is lower than the peak value of the uncoordinated charging method that satisfies the maximum SOC demand of EVs. To avoid the new charging peak load of the microgrid in the coordinated plan, a constraint for the microgrid shown in Eq. (17) should be added to restrict the increase of the peak value [33].

$$P_{T-c}^{\max} \le P_{T-uc(\max SOC)}^{\max} \tag{17}$$

where $P_{T-uc(\max SOC)}^{\max}$ is the maximum of the total load in the uncoordinated charging method that satisfies the maximum SOC demand of EVs in 96 time slots.

3.7. Total load of microgrid

The charging scheduling results can be obtained by solving the proposed optimization model. Moreover, the effect of the coordinated charging scheduling method can be verified by contrasting the coordinated charging method and uncoordinated charging methods.

Fig. 4 and Fig. 5 are the processes for calculating the total load in the uncoordinated and coordinated charging methods, respectively. In Eq. (15), the SOC of normal charging EVs when they are disconnected from the microgrid should be between the minimum and maximum SOC demand in the coordinated charging method. In the uncoordinated charging methods, the experiment will be conducted twice to meet the minimum and maximum SOC demand for EVs. Then, the total load in each time slot of the three charging situations can be obtained.

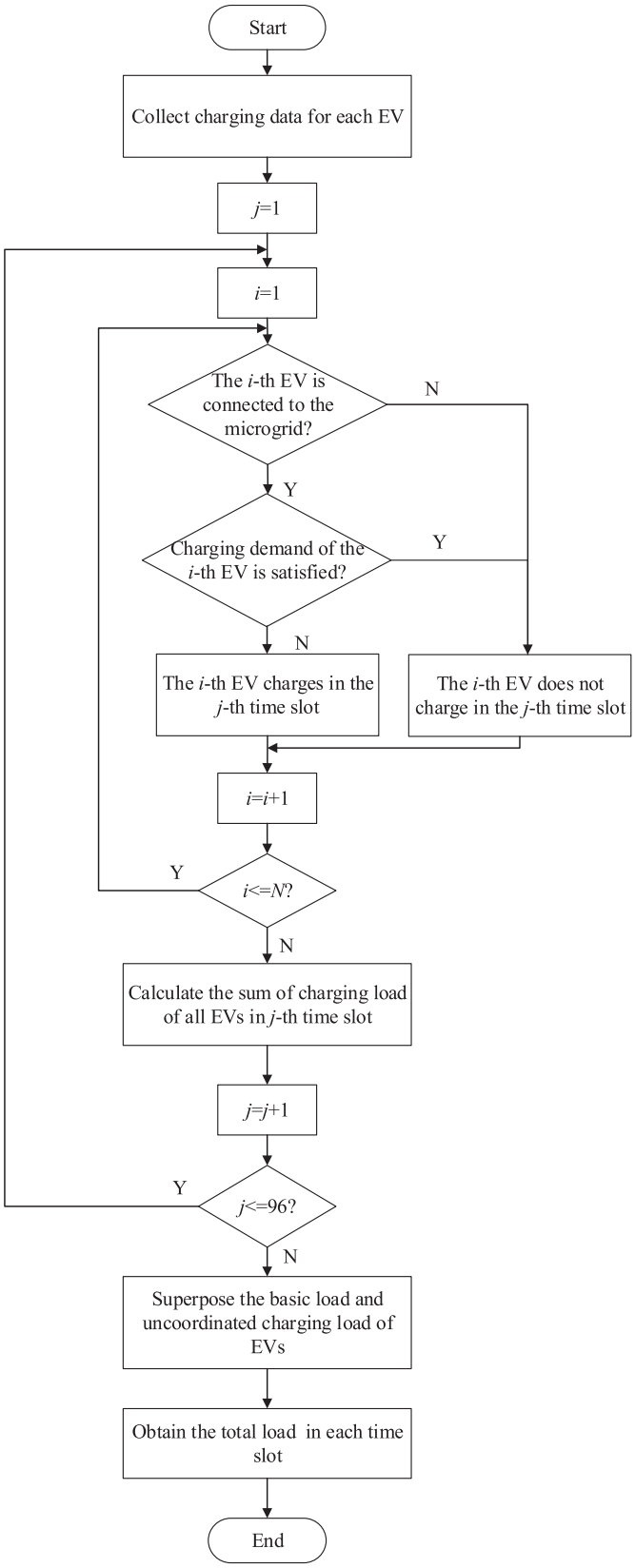

Fig. 4. Calculation process of total load in uncoordinated charging method.

4. Results and discussions

4.1. Simulation data and setup

The proposed model was built in MATLAB/YALMIP and solved by CPLEX solver. The input data in the experiment are generated randomly according to the probability density function to simulate the real EV charging situations. Nevertheless, some assumptions have to be established for simplicity.

First, different number of EVs (i.e., 100, 200, and 300) were used for comparative experiments. Meanwhile, the experiment assumed

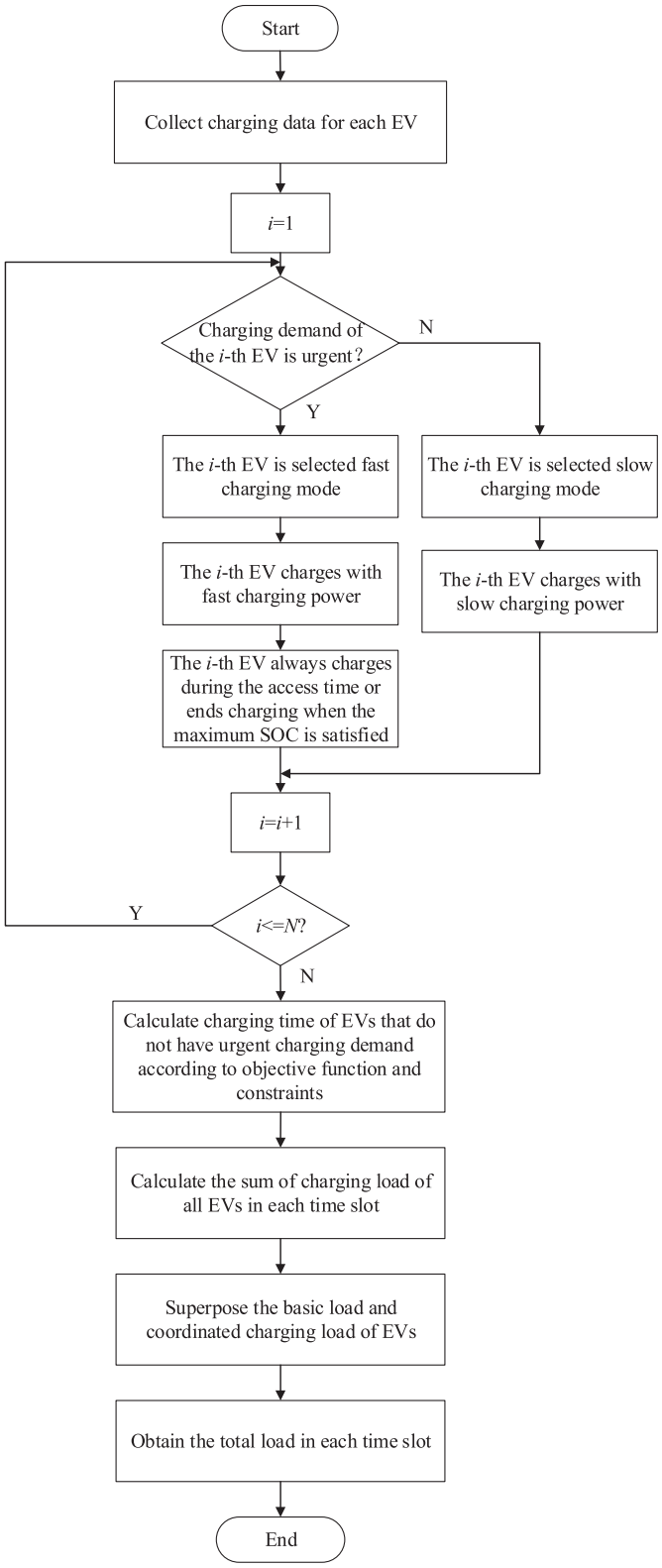

Fig. 5. Calculation process of total load in proposed coordinated charging method.

that there are different numbers of EVs charging in the home-charging and public-charging patterns. In the simulation, the stochastic data of the charging and discharging time for the different numbers of EVs in the two charging patterns are obtained as shown in Figs. 2 and 3.

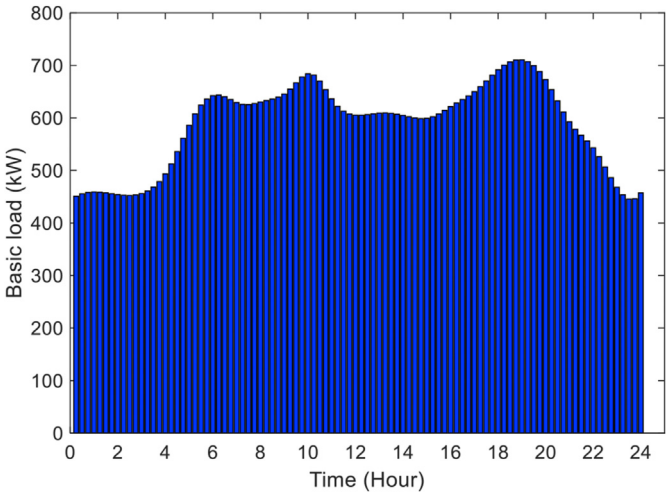

Fig. 6. Typical basic load profile in one-day cycle.

Second, SOC_i^{con} were assumed to follow the continuous uniform distribution between 0.1 and 0.3. $SOC_i^{\min}$ is given by uniform distribution between 0.4 and 0.6, and $SOC_i^{\max}$ is given by uniform distribution between 0.8 and 1.0 [8,33]. P_{EV}^{slow} and P_{EV}^{fast} are set to 3.5 kW and 10 kW, η_{EV} is set to 0.9. Moreover, the capacity of all EV batteries Cap_{EV}^{bat} is set to 30 kWh [34].

Finally, the basic load data have been simulated according to the pattern of electricity usage [33]. The simulation results are shown in Fig. 6, which illustrates the typical basic load profile of the regional microgrid in a day-cycle scenario. The peak hours occur at approximately 6 h, 10 h, and 18 h. The highest load is 710.62 kW, the lowest load is 445.69 kW.

4.2. Scheduling results and comparative analysis

4.2.1. Home-charging pattern

In the home-charging pattern, the EV owners are accustomed to charge in the night and drive in the next day. In the experiment, the one-day cycle is contained by two half-days. To present whole scheduling process of the EV charging, the 12 h time of one day to the 12 h time of the next day is chosen as the scheduling time period, and 15 min is defined as one time slot that divides a one-day cycle into 96 equal parts.

The simulation results of EV optimal charging scheduling with three different charging methods in the home-charging pattern are shown in Fig. 7. In each figure, three different charging scheduling strategies are employed. And 96 time slots have been presented by histograms in each figure. For these uncoordinated charging scheduling plans, the EV charges begin with the arrival time slot. Moreover, the EV stays in the charge state all of the time until the departure time slot or the time slot that the maximum SOC demand of the EV owner is satisfied. Because both the minimum SOC and maximum SOC demand have been considered in this model, the two kinds of charging SOC in uncoordinated charging scheduling methods should be considered in uncoordinated charging scheduling methods.

For EVs that have urgent charging demand, parts of the EV charging time are too short, so the uncoordinated charging strategies cannot ensure the minimum SOC demand of EVs can be satisfied in such an urgent situation. However, the urgent charging situation can be handled when adopting the coordinated charging scheduling method. For slow-charging EVs, conditions ensure that

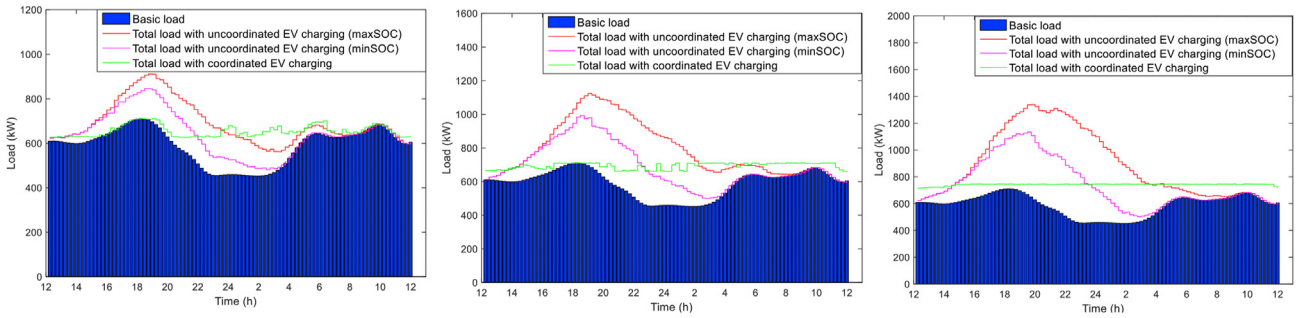

Fig. 7. Results of uncoordinated charging and the proposed coordinated charging in home-charging pattern.

Table 1
Comparison of three profiles in home-charging pattern.

Number of EV		100	200	300
Peak value (kW)	UC (max SOC)	911.35	1123.40	1331.80
	UC (min SOC)	846.15	993.15	1107.80
	C	710.91	710.91	750.90
Valley value (kW)	UC (max SOC)	562.42	597.31	604.31
	UC (min SOC)	480.99	499.69	506.82
	C	626.93	660.31	675.02
Range (kW)	UC (max SOC)	348.93	526.12	727.51
	UC (min SOC)	365.16	493.46	601.00
	C	83.98	50.60	75.88
Variance	CON	6588.80	6588.80	6588.80
	UC (max SOC)	8967.70	25,758.00	59,316.00
	UC (min SOC)	9628.40	16, 921.00	31,022.00
	C	690.57	346.99	270.67

Table 2
Effect of the coordinated charging method on peak shaving and valley filling in home-charging pattern.

Number of EV		100	200	300
Change of peak value	UC (max SOC)	−21.99%	−36.72%	−43.62%
	UC (min SOC)	−15.98%	−28.42%	−32.22%
Change of valley value	UC (max SOC)	+11.47%	+10.55%	+11.70%
	UC (min SOC)	+30.34%	+32.14%	+33.19%
Change of range	UC (max SOC)	−75.93%	−90.38%	−89.57%
	UC (min SOC)	−77.00%	−89.75%	−87.37%
Change of variance	UC (max SOC)	−92.30%	−98.65%	−99.54%
	UC (min SOC)	−92.83%	−97.95%	−99.13%

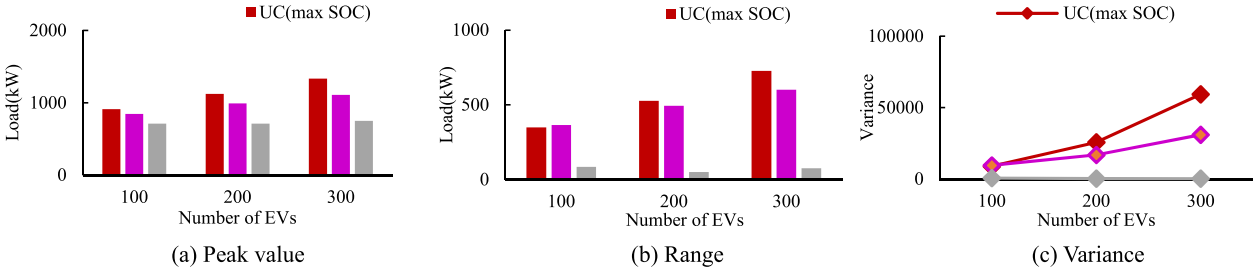

Fig. 8. Comparison of three methods in home-charging pattern.

the SOC when EVs are disconnected from microgrid should be between the upper and lower demand of the SOC. Therefore, the entirety of EVs charging power from the microgrid in the coordinated situation is lower than that of the uncoordinated charging scheduling that satisfies the maximum SOC demand but higher than that of the uncoordinated charging scheduling that satisfies the minimum SOC demand. As Fig. 7 shows, the charging profile of the coordinated method is gentler than the two uncoordinated charging profiles. The three profiles in the home-charging pattern are compared in Table 1.

In Table 1, UC (max SOC) and UC (min SOC) mean the uncoordinated EV charging scheduling method that satisfies the

maximum and minimum SOC demand, respectively. C is coordinated EV charging scheduling method. As shown in Table 1, compared to the two uncoordinated charging scheduling methods, the coordinated charging scheduling method can reduce the peak value, range and variance of the total load. Furthermore, to compare the effect of the coordinated charging method in the different situations, the indexes of the coordinated charging in Table 1 should be contrasted in Table 2. The coordinated charging method and uncoordinated charging methods are compared according to the three aspects in Fig. 8.

In Fig. 8 (a), compared to the uncoordinated charging that satisfies the maximum SOC demand, the coordinated charging method can reduce the peak value by 21.99%, 36.72% and 43.62% with 100, 200 and 300 EVs, respectively. In addition, compared to the uncoordinated charging that satisfies the minimum SOC demand, the coordinated charging method can reduce the peak value by 15.98%, 28.42% and 32.22%, respectively.

In Fig. 8 (b), the range of total load with the uncoordinated charging that satisfies the maximum SOC demand can be reduced 75.93%, 90.38% and 89.57%, respectively, by the coordinated charging scheduling method in the three charging scales. Similarly, the range of the uncoordinated charging that satisfies the minimum SOC demand can be reduced by 77%, 89.75% and 87.37%, respectively.

In Fig. 8 (c), unlike the uncoordinated charging method that satisfies the maximum SOC demand, employing the coordinated charging scheduling method can reduce the variance of the total load by 92.30%, 98.65%, and 99.54% in the three EV scales. In addition, the variance of uncoordinated charging method that satisfies the minimum SOC demand can be reduced by 92.83%, 97.95% and 99.13%, respectively.

4.2.2. Public-charging pattern

In the public-charging pattern, a cycle is defined as ranging from 0 h to 24 h in a day. The simulation results are shown in Fig. 9. For all EVs involved, it can be seen that the demand surges at approximately 10 h when the uncoordinated charging method was employed. The statistical data in the public-charging pattern are shown in Table 3.

As Table 3 shows, the coordinated charging scheduling plan can reduce the peak value, range and variance of the total load, which makes the total load profile of the microgrid gentler when compared to the two uncoordinated charging methods. Similar to the home-charging pattern, the indexes of coordinated charging in Table 3 can be contrasted to the two uncoordinated charging methods in the three situations in which different numbers of EVs are involved. The comparison results are presented in Table 4 and Fig. 10.

In Fig. 10 (a), compared to the uncoordinated charging that satisfies the maximum SOC demand, the coordinated charging method can reduce the peak value by 18.95%, 26.84% and 34.93% in the three EV scales. Moreover, the peak load values of uncoordinated charging that satisfies the minimum SOC demand can be reduced by 10.90%, 15.39% and 20.27%, respectively, with the different numbers of EVs.

As Fig. 10 (b) shows, the range of the uncoordinated charging that satisfies the maximum SOC demand can be reduced by 42.74%, 49.27% and 56.12%, and the uncoordinated charging that satisfies the minimum SOC demand can be cut down 30.11%, 35.18% and 39.95% by the coordinated charging scheduling method in the three EV scales. Moreover, when more EVs are involved, the function that reduces the peak-valley load difference is more apparent in the public-charging pattern.

In Fig. 10 (c), unlike the uncoordinated charging method that satisfies the maximum SOC demand, employing the coordinated charging scheduling method can reduce the variance of the total load by 52.82%, 65.81%, and 73.65% in the three EV scales. In addition, the variance of total load of the uncoordinated charging method that satisfies the minimum SOC demand can be reduced by 20.35%, 28.10% and 38.36%, respectively.

The differences between the coordinated charging and two uncoordinated charging approaches in the total load of the microgrid are discussed above. However, the effect of the three charging methods on the basic load has not been analysed. Therefore, the effect of the three charging methods on the variance of the basic load in the two patterns is presented in Fig. 11.

Fig. 11 (a) shows the uncoordinated EV charging can increase the fluctuation of the microgrid operation in the home-charging pattern. In contrast, the coordinated charging scheduling method can reduce the variance of the basic load by 90%, 95% and 96% in the three EV scales.

From Fig. 11 (b), it can be found that the three charging methods can all increase the variance of the basic load and fluctuation of the microgrid. However, compared to the uncoordinated charging methods, the negative effect of the coordinated scheduling charging method is much smaller than that of the two uncoordinated charging methods.

4.3. The impact of charging pattern

According to the analysis of the effect of the three charging methods on the variance of the basic load of the microgrid, the two charging patterns show different effects on peak shaving and valley filling. The coordinated charging scheduling plan can reduce the variance of the basic load when EVs are connected to the microgrid in the home-charging pattern. However, the EV charging can

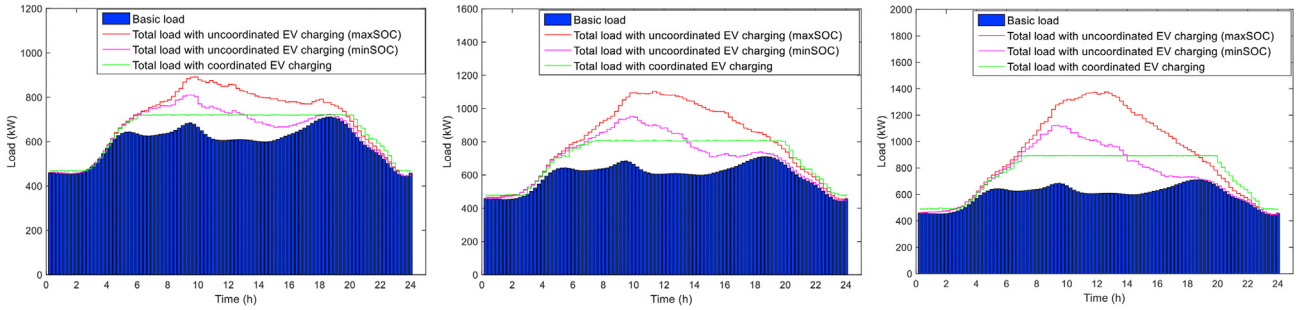

(a) 100 EVs (b) 200 EVs (c) 300 EVs

Fig. 9. Results of uncoordinated charging and the proposed coordinated charging in public-charging pattern.

Table 3
Comparison of three profiles in public-charging pattern.

Number of EVs		100	200	300
Peak value (kW)	UC (max SOC)	891.67	1104.10	1375.50
	UC (min SOC)	811.06	954.67	1122.60
	C	722.67	807.77	895.04
Valley value (kW)	UC (max SOC)	445.38	453.38	448.88
	UC (min SOC)	445.38	445.38	445.38
	C	467.11	477.67	488.38
Range (kW)	UC (max SOC)	446.30	650.68	926.64
	UC (min SOC)	365.68	509.30	677.18
	C	255.56	330.10	406.66
Variance	CON	6073.60	6073.60	6073.60
	UC (max SOC)	21,098.00	48,396.00	101,700.00
	UC (min SOC)	12,497.00	23,017.00	43,473.00
	C	9953.30	16,549.00	26,796.00

Table 4
Effect of the coordinated charging method on peak shaving and valley filling in public-charging pattern.

Number of EVs		100	200	300
Change of peak value	UC (max SOC)	−18.95%	−26.84%	−34.93%
	UC (min SOC)	−10.90%	−15.39%	−20.27%
Change of valley value	UC (max SOC)	+4.88%	+5.36%	+8.80%
	UC (min SOC)	+4.88%	+7.25%	+9.66%
Change of range	UC (max SOC)	−42.74%	−49.27%	−56.12%
	UC (min SOC)	−30.11%	−35.18%	−39.95%
Change of variance	UC (max SOC)	−52.82%	−65.81%	−73.65%
	UC (min SOC)	−20.35%	−28.10%	−38.36%

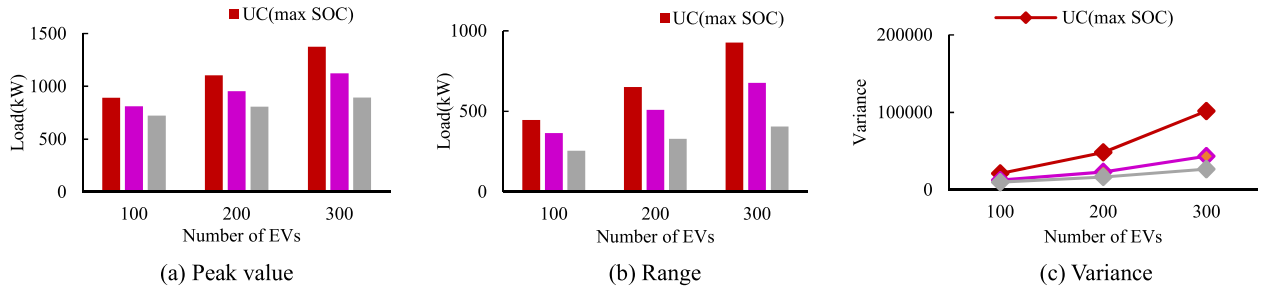

Fig. 10. Comparison of three methods in public-charging pattern.

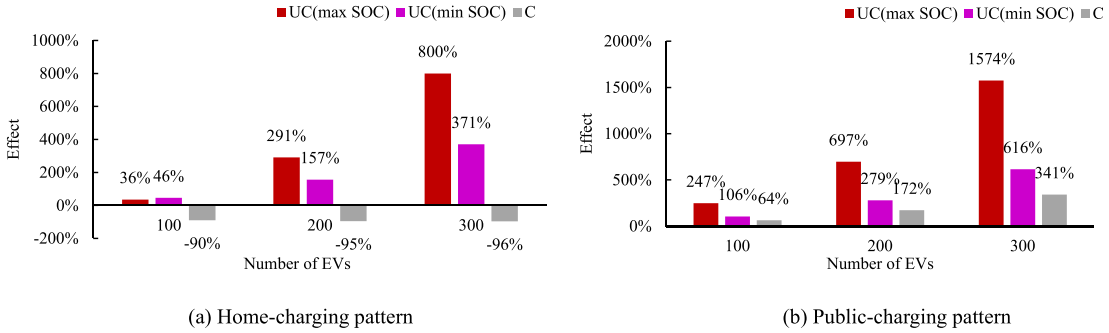

Fig. 11. Effect of three charging methods on the variance of basic load in two patterns.

increase the variance of the basic load in the public-charging pattern. Moreover, the coordinated charging profiles of Fig. 7 are gentler than the coordinated charging profiles of Fig. 9 in the three charging scales. The reasons for this phenomenon are discussed in the following.

First, the average detention time of EVs in home-charging is longer than that in the public-charging pattern. In the home-charging pattern, the EVs are connected to the microgrid at approximately 18 h and disconnected from microgrid approximately 8 h. However, in the public-charging pattern, EVs tend to be connected to the microgrid at approximately 8.5 h and disconnected at 17.5 h.

Moreover, in the home-charging pattern, the peak value of the basic load occurs at 18 h, 5 h, and 10 h, and the value of the valley

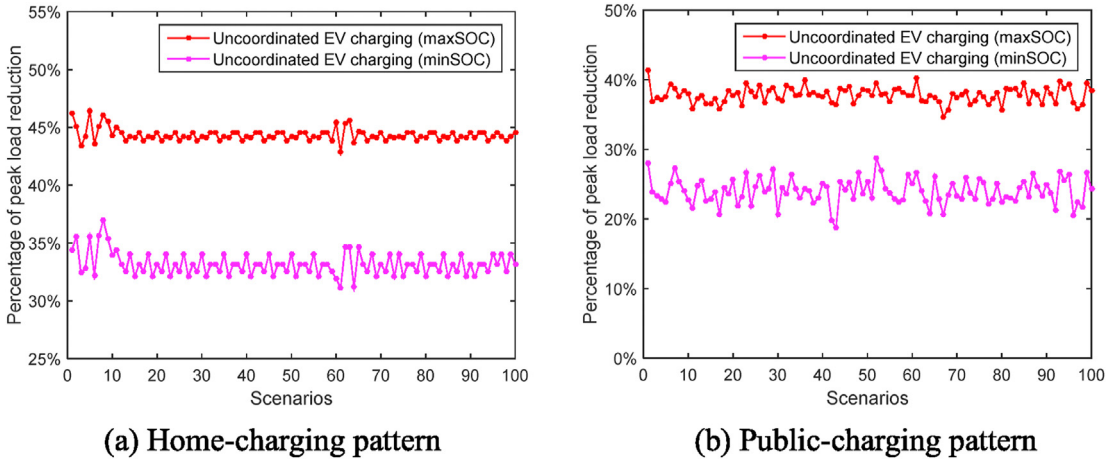

Fig. 12. Effect of coordinated charging method on peak shaving under 100 scenarios.

occurs during 23 h–4 h. In addition, most EVs in this model are connected to the microgrid at approximately 18 h and disconnected at around 8 h, so the value of the valley of the basic load can be filled in most of the EV charging time. Furthermore, the peak load pressure can be decreased, and the peak-shaving and valley-filling effects are obvious.

In public-charging, the peak value of the basic load occurs at 5 h, 10 h and 18 h and the value of the valley occurs during 23 h–4 h. However, in this pattern, most EVs are connected to the microgrid at approximately 8.5 h and disconnected at approximately 17.5 h. Therefore, the value of the valley of the basic load can only be filled by a few EVs because the most EV charging time misses the valley time of the basic load. For coordinated charging scheduling, the valley time cannot be used adequately, which influences the effect of the coordinated charging scheduling plan on peak shaving and valley filling.

The proposed coordinated charging method has an advantage over the uncoordinated charging method in regard to relieving the peak load pressure in the microgrid operation, while this advantage of the proposed coordinated method can satisfy the urgent charging demand.

4.4. Validation of the simulation results

To evaluate the effectiveness of the proposed coordinated charging method, 100 scenarios have been simulated with 300 EVs in two charging patterns. The input data were generated stochastically based on the method described in Section 4.1. In the evaluation part, the coordinated charging method is compared to two different uncoordinated charging methods in terms of the peak load and variance, and the results are shown in Fig. 12 and Fig. 13.

In each figure of Fig. 12, the two profiles refer to percentages of peak load reduction through the coordinated charging method when compared to the uncoordinated charging method that satisfies the maximum and minimum SOC demand. Moreover, in each figure of Fig. 13, the two profiles refer to the percentages of variance reduction through the coordinated charging method when compared to the uncoordinated charging method that satisfies the maximum and minimum SOC demand.

In Fig. 12 (a), compared to the uncoordinated charging methods that satisfy the minimum SOC and maximum SOC demand, the coordinated charging method could reduce the peak load of the microgrid by approximately 45% and 32%, respectively, under different scenarios in the home-charging pattern. As Fig. 13 (a) shows, the variance of the microgrid with uncoordinated charging methods can be reduced by the coordinated charging method by approximately 99.5%. Similarly, in the public-charging pattern, the peak load of the uncoordinated charging methods has been reduced by approximately 37% and 25% in Fig. 12 (b). In addition, the variance has been reduced by an average of approximately 80%

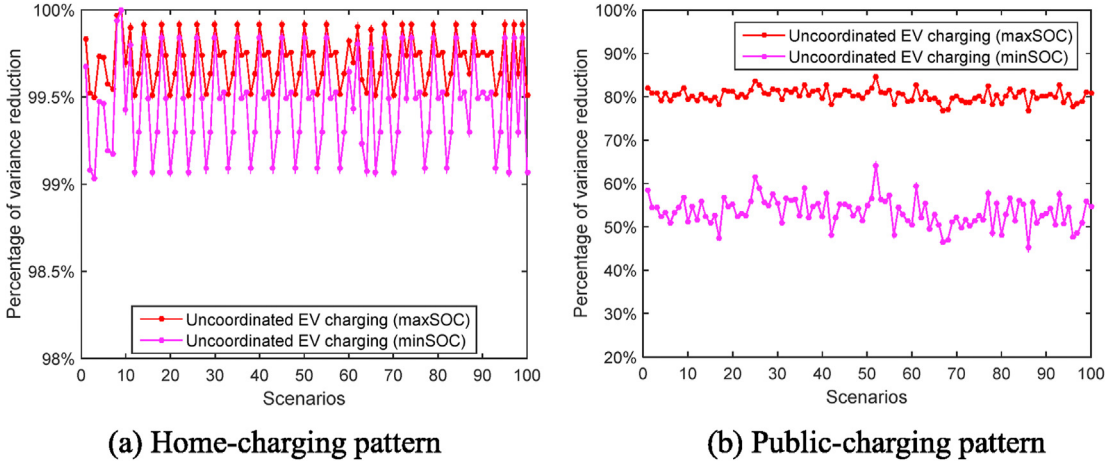

Fig. 13. Effect of coordinated charging method on load fluctuation relieving under 100 scenarios.

and 50% in Fig. 13 (b).

After comparing the coordinated charging method with uncoordinated charging methods, the peak-shaving function and load fluctuation-relieving function were evaluated. Moreover, the additional 100 scenarios in the two charging patterns verify that the validity of coordinated charging methods and results of previous simulation experiments are trustworthy.

5. Conclusions

This study proposed a coordinated charging scheduling method for EVs by considering the urgent charging demand of EV owners. In the charging scheduling process, all the EVs are scheduled according to different groups instead of scheduled as a whole. Two charging patterns were considered in the experiment to illustrate the effect of the method on peak shifting and valley filling. Moreover, three groups of EV scales were applied in the experiments to test the effectiveness of the method. Finally, the simulation was implemented 100 times, and the two charging patterns with 300 EVs were used to evaluate the effectiveness of the proposed method.

In addition, the method considered the peak-shifting and valley-filling effects on the microgrid. The advantage of this study is that the proposed method simultaneously achieves charging mode selection of EVs that have different charging demand and microgrid operation improvement.

In future work, more influence factors will be considered for the EV coordinated charging scheduling.

Author statement

Kaile Zhou: Conceptualization, Methodology, Resources, Visualization, Writing- Reviewing and Editing, Project administration, Supervision. **Lexin Cheng**: Conceptualization, Methodology, Data curation, Software, Visualization, Formal analysis, Writing- Original draft preparation. **Lulu Wen**: Methodology, Writing- Reviewing and Editing. **Xinhui Lu:** Visualization, Writing- Reviewing and Editing. **Tao Ding:** Supervision.

Declaration of competing interest

The authors declare that they have no known competing financial interests or personal relationships that could have appeared to influence the work reported in this paper.

Acknowledgments

This work is supported by the National Natural Science Foundation of China (Nos. 71822104 and 71521001), and the Fundamental Research Funds for the Central Universities (No. JZ2018HGPA0271).

References

[1] Martínez-Lao J, Montoya FG, Montoya MG, Manzano-Agugliaro F. Electric vehicles in Spain: an overview of charging systems. Renew Sustain Energy Rev 2016;77:970–83.
[2] Miao R, Huang W, Pei D, Gu X, Li Z, Zhang J, Jiang Z. Research on lease and sale of electric vehicles based on value engineering. Int J Prod Res 2016;54(18):5361–80.
[3] Nunes P, Brito MC. Displacing natural gas with electric vehicles for grid stabilization. Energy 2018;141:87–96.
[4] de Mello Bandeira RA, Goes GV, Gonçalves DNS, Márcio de Almeida DA, de Oliveira CM. Electric vehicles in the last mile of urban freight transportation: a sustainability assessment of postal deliveries in Rio de Janeiro-Brazil. Transport Res Transport Environ 2019;67:491–502.
[5] Gopal AR, Park WY, Witt M, Phadke A. Hybrid- and battery-electric vehicles offer low-cost climate benefits in China. Transport Res Transport Environ 2018;62:362–71.
[6] Kumar MS, Revankar ST. Development scheme and key technology of an electric vehicle: an overview. Renew Sustain Energy Rev 2016;70:1266–85.
[7] Teixeira ACR, Silva DLD, Diniz ASAC, Sodré JR. A review on electric vehicles and their interaction with smart grids: the case of Brazil. Clean Technol Environ Policy 2015;17(4):841–57.
[8] Jian L, Zheng Y, Shao Z. High efficient valley-filling strategy for centralized coordinated charging of large-scale electric vehicles. Appl Energy 2017;186(part_P1):46–55.
[9] Benabdelaziz K, Maaroufi M. Battery dynamic energy model for use in electric vehicle simulation. Int J Hydrogen Energy 2017;42(30):19496–503.
[10] Han S, Han S, Aki H. A practical battery wear model for electric vehicle charging applications. Appl Energy 2014;113(6):1100–8.
[11] Wang D, Coignard J, Zeng T, Zhang C, Saxena S. Quantifying electric vehicle battery degradation from driving vs. vehicle-to-grid services. J Power Sources 2016;332:193–203.
[12] Zhao Y, Liu P, Wang Z, Zhang L, Hong J. Fault and defect diagnosis of battery for electric vehicles based on big data analysis methods. Appl Energy 2017;207:354–62.
[13] González LG, Siavichay E, Espinoza JL. Impact of EV fast charging stations on the power distribution network of a Latin American intermediate city. Renew Sustain Energy Rev 2019;107:309–18.
[14] Levinson RS, West TH. Impact of public electric vehicle charging infrastructure. Transport Res Transport Environ 2017;64:158–77.
[15] Domínguez-Navarro JA, Dufo-López R, Yusta-Loyo JM, Artal-Sevil JS, Bernal-Agustín JL. Design of an electric vehicle fast-charging station with integration of renewable energy and storage systems. Int J Electr Power Energy Syst 2018;105:46–58.
[16] Elsayad N, Mohammed OA. A cascaded high frequency AC link system for large-scale PV-assisted EV fast charging stations. In: Transportation electrification conference & expo; 2017. p. 90–4.
[17] Wu S-M, Liu H-C, Wang L-E. Hesitant fuzzy integrated MCDM approach for quality function deployment: a case study in electric vehicle. Int J Prod Res 2017;55(15):4436–49.
[18] Zhen L, Xu Z, Ma C, Xiao L. Hybrid electric vehicle routing problem with mode selection. Int J Prod Res 2019:1–15.
[19] Qian K, Zhou C, Allan M, Yuan Y. Modeling of load demand due to EV battery charging in distribution systems. IEEE Trans Power Syst 2011;26(2):802–10.
[20] Luo Y, Zhu T, Wan S, Zhang S, Li K. Optimal charging scheduling for large-scale EV (electric vehicle) deployment based on the interaction of the smart-grid and intelligent-transport systems. Energy 2016;97:359–68.
[21] Guo C, Chan CC. Analysis method and utilization mechanism of the overall value of EV charging. Energy Convers Manag 2015;89:420–6.
[22] Sassi O, Oulamara A. Electric vehicle scheduling and optimal charging problem: complexity, exact and heuristic approaches. Int J Prod Res 2017;55(2):519–35.
[23] Sousa T, Morais H, Soares J, Vale Z. Day-ahead resource scheduling in smart grids considering Vehicle-to-Grid and network constraints. Appl Energy 2012;96:183–93.
[24] Gharesifard B, Basar T, Dominguez-Garcia AD. Price-based distributed control for networked plug-in electric vehicles. In: American control conference; 2013. p. 5086–91.
[25] Ma Z, Callaway DS, Hiskens IA. Decentralized charging control of large populations of plug-in electric vehicles. IEEE Trans Contr Syst Technol 2012;21(1):67–78.
[26] Zhan K, Hu Z, Song Y, Lu N, Xu Z, Jia L. A probability transition matrix based decentralized electric vehicle charging method for load valley filling. Elec Power Syst Res 2015;125:1–7.
[27] Zhang K, Xu L, Ouyang MH, Lu L, Li J, Li Z. Optimal decentralized valley-filling charging strategy for electric vehicles. Energy Convers Manag 2014;78(2):537–50.
[28] Giorgio AD, Liberati F. Near real time load shifting control for residential electricity prosumers under designed and market indexed pricing models. Appl Energy 2014;128(128):119–32.
[29] Liu D, Xiao B. Exploring the development of electric vehicles under policy incentives: a scenario-based system dynamics model. Energy Pol 2018;120:8–23.
[30] Zhang T, Pota H, Chu CC, Gadh R. Real-time renewable energy incentive system for electric vehicles using prioritization and cryptocurrency. Appl Energy 2018;226:582–94.
[31] Pearre NS, Swan LG. Electric vehicle charging to support renewable energy integration in a capacity constrained electricity grid. Energy Convers Manag 2016;109:130–9.
[32] Schuller A, Flath CM, Gottwalt S. Quantifying load flexibility of electric vehicles for renewable energy integration. Appl Energy 2015;151(August 2015):335–44.
[33] Zheng Y, Shang Y, Shao Z, Jian L. A novel real-time scheduling strategy with near-linear complexity for integrating large-scale electric vehicles into smart grid. Appl Energy 2018;217:1–13.
[34] Jian L, Zheng Y, Xiao X, Chan CC. Optimal scheduling for vehicle-to-grid operation with stochastic connection of plug-in electric vehicles to smart grid. Appl Energy 2015;146:150–61.
[35] Jian L, Zhu X, Shao Z, Niu S, Chan CC. A scenario of vehicle-to-grid implementation and its double-layer optimal charging strategy for minimizing load variance within regional smart grids. Energy Convers Manag 2014;78(2):

508–17.
[36] Oliveira DQ, Zambroni dSAC, Delboni LFN. Optimal plug-in hybrid electric vehicles recharge in distribution power systems. Elec Power Syst Res 2012;98(5):77–85.
[37] Al-Awami AT, Sortomme E. Coordinating vehicle-to-grid services with energy trading. IEEE Trans Smart Grid 2012;3(1):453–62.
[38] Shi L, Qian Z, Pu Y. The reserve trading model considering V2G. Rever Energy 2013;59(C):50–5.
[39] El-Zonkoly A. Intelligent energy management of optimally located renewable energy systems incorporating PHEV. Energy Convers Manag 2014;84:427–35.
[40] Fazelpour F, Vafaeipour M, Rahbari O, Rosen MA. Intelligent optimization to integrate a plug-in hybrid electric vehicle smart parking lot with renewable energy resources and enhance grid characteristics. Energy Convers Manag 2014;77(1):250–61.
[41] White CD, Zhang KM. Using vehicle-to-grid technology for frequency regulation and peak-load reduction. J Power Sources 2011;196(8):3972–80.
[42] Sheikhi A, Bahrami S, Ranjbar AM, Oraee H. Strategic charging method for plugged in hybrid electric vehicles in smart grids; a game theoretic approach. Int J Electr Power Energy Syst 2013;53(1):499–506.
[43] Bai X, Qiao W, Wei H, Huang F, Chen Y. Bidirectional coordinating dispatch of large-scale V2G in a future smart grid using complementarity optimization. Int J Electr Power Energy Syst 2015;68:269–77.
[44] Saber AY, Venayagamoorthy GK. Plug-in vehicles and renewable energy sources for cost and emission reductions. IEEE Trans Ind Electron 2011;58(4):1229–38.
[45] Su W, Chow MY. Computational intelligence-based energy management for a large-scale PHEV/PEV enabled municipal parking deck. Appl Energy 2012;96(8):171–82.
[46] Yang J, He L, Fu S. An improved PSO-based charging strategy of electric vehicles in electrical distribution grid. Appl Energy 2014;128(3):82–92.
[47] Lunz B, Walz H, Sauer DU. Optimizing vehicle-to-grid charging strategies using genetic algorithms under the consideration of battery aging. In: IEEE vehicle power & propulsion conference; 2011. p. 7.
[48] Xu M, Meng Q, Liu K, Yamamoto T. Joint charging mode and location choice model for battery electric vehicle users. Transp Res Part B Methodol 2017;103:68–86.